ADVANCED LIFETIME SPECTROSCOPY – METHODOLOGY AND EXPERIMENTAL PROOF

S. Rein and S.W. Glunz
Fraunhofer Institute for Solar Energy Systems ISE, Heidenhofstr. 2, D-79110 Freiburg, Germany
Phone ++49 761-4588-5271; Fax ++49 761-4588-9000, email: stefan.rein@ise.fraunhofer.de

ABSTRACT: Lifetime spectroscopy (LS) always allows a complete defect characterization on one single sample if data from injection- and temperature-dependent LS (TDLS and IDLS) are combined. To allow an accurate modeling of entire TDLS curves, several physical extensions are introduced in the basic Shockley-Read-Hall (SRH) model. A new routine for data evaluation allows a transparent SRH analysis of IDLS and TDLS data and makes it possible to assess the accuracy and consistency of the determined defect parameters. Applied to LS data from a molybdenum-contaminated silicon sample, the advanced lifetime spectroscopy allows the identification of a known molybdenum donor level at E_t-E_V=0.317 eV with an enhanced electron/hole capture cross section ratio k:=σ_n/σ_p=13. The good agreement with literature and the consistency of the LS results manifest the potential of the proposed advanced LS analysis. If the value for σ_p is taken from literature, the unknown electron capture cross section of the molybdenum donor level is determined as σ_n=7.8×10^{-15} cm^2.

Keywords: Lifetime, Spectroscopy, Defects.

1. INTRODUCTION

Although deep-level transient spectroscopy (DLTS) is accepted to be one of the most sensitive methods to detect and analyze small concentrations of electrically active defects, defect concentrations below the detection limit of DLTS can still significantly affect carrier recombination lifetime. Apart from detecting the presence of recombination-active defects, lifetime measurements allow a direct identification of defects if the injection and temperature dependence of carrier lifetime is analyzed on the basis of standard Shockley-Read-Hall (SRH) theory [1, 2]. Recently, Rein et al. [3] have demonstrated that lifetime spectroscopy (LS) *always* allows a complete defect characterization on one single sample if the data from temperature-dependent and injection-dependent lifetime spectroscopy (TDLS and IDLS) are combined. Furthermore, it has been shown that *often* the modeling of the entire TDLS curve alone allows an unambiguous determination of both, the ratio k:=σ_n/σ_p of the capture cross sections for electrons and holes and the exact energy position E_t within the band gap [3]. The recent successful decoding of the electronic structure of the well-known metastable defect in Czochralski silicon demonstrates the potential of this advanced lifetime spectroscopy [4].

In the present work further extensions of the LS analysis are presented. On the one hand the basic SRH model is extended to allow an accurate simulation of TDLS curves in an extended temperature range from 130 to 580 K. On the other hand a new routine for data evaluation, which we introduced only recently [4], is further extended and improved: the determination of the *defect-parameter-solution-surface* (DPSS). In order to demonstrate the potential of this advanced LS for a detailed and complete defect characterization, we performed TDLS and IDLS measurements on an intentionally molybdenum-contaminated *p*-type silicon sample.

2. ADVANCED TDLS ANALYSIS

Figure 1 shows the TDLS curve of the Mo-contaminated sample which has been measured under low-level injection (LLI) by means of the contactless microwave-detected photoconductance decay technique (MWPCD) (for experimental details see Ref. [2]). As surface recombination is effectively suppressed by the use of a high-quality SiN surface passivation (S<20 cm/s in the whole T- and Δn-range), the measured effective carrier lifetime directly reflects SRH recombination via the molybdenum centers in the bulk.

2.1. Superposed effects: extensions of the SRH model

If the advanced TDLS analysis is applied, the accuracy of defect parameter determination strongly depends on the accuracy of the SRH fit. To allow a comprehensive verification of the validity of SRH theory, the investigated T-range has been significantly increased from 200-500 K in all previous studies to 130-580 K in the present study, as partly shown in Fig. 1. The dashed line shows a least squares optimization of the *basic SRH model* whose T-dependence arises from only three quantities: the SRH densities $n_1(T)$, $p_1(T)$, the densities of states $N_C(T)$, $N_V(T)$ and the thermal velocity $v_{th}(T)$. As can be seen, basic SRH theory fails to describe the observed T-dependence in the whole T-range. While an adequate description is achieved under medium temperatures from 250-500 K, strong deviations are observed above 500 K and below 250 K.

We first focus on the correct modeling of the *low-temperature part* of the TDLS curve. For temperatures below the onset of the Arrhenius increase (here: T<250 K), SRH lifetime under low-level injection equals the minority capture time constant τ_{n0}:=$[N_t\sigma_n(T)v_{th}(T)]^{-1}$. Thus, all deviations from the known temperature dependence of v_{th} (thin dashed line in Fig. 1) have to be attributed to a temperature dependence of the minority carrier capture cross section. The observed decrease of the capture cross section with increasing temperature can be modeled in terms of $\sigma(T)=\sigma_0 T^{\alpha}$ with an exponent α = -1.5 (thin solid line). Such a $\sigma(T)$-model either points towards a cascade capture process [5], which is only found for shallow Coulomb attractive centers, or towards an excitonic Auger capture process [6], which is observed for centers of arbitrary depth and charge state. As the cascade mechanism is unlikely due to an energy depth of 0.32 eV of the underlying defect center (see below), the excitonic Auger mechanism is likely to be the dominating process. The fact that precisely the same T-dependence has been identified on a second Mo-contaminated sample, demonstrates its significance as an

additional fingerprint of the defect center which elucidates the physical mechanism of carrier capture.

Whether the underlying $\sigma(T)$-model is considered or not leads to a fundamental difference in fitting the linear Arrhenius increase. As shown by the dashed lines in Fig. 1, the basic SRH model with temperature-independent capture cross sections only allows a correct modeling of the Arrhenius increase for a MinBH defect (defect in the upper band gap half in *p*-type) while that for a MajBH defect (defect in the lower band gap half in *p*-type) fails. This is reflected in a Chi^2-value which is increased by more than an order of magnitude for the MajBH fit compared to the MinBH fit. From this observation we concluded in a previous work [3] that the relevant defect level of molybdenum is located in the upper half of the band gap. Nevertheless, if the $\sigma(T)$-model extracted from the low-temperature part of the TDLS curve is introduced into the SRH analysis, the electron capture time constant $\tau_{n0}(T)$ – being a scaling factor of SRH lifetime – exhibits a slight increase with increasing temperature (thin solid line), which allows an accurate modeling of the linear Arrhenius increase for a MinBH *and* a MajBH defect with an energy depth of 0.31 eV (dash-dotted lines in Fig. 1). Since the fit quality is more or less the same, an unambiguous identification of the band gap half is no longer possible.

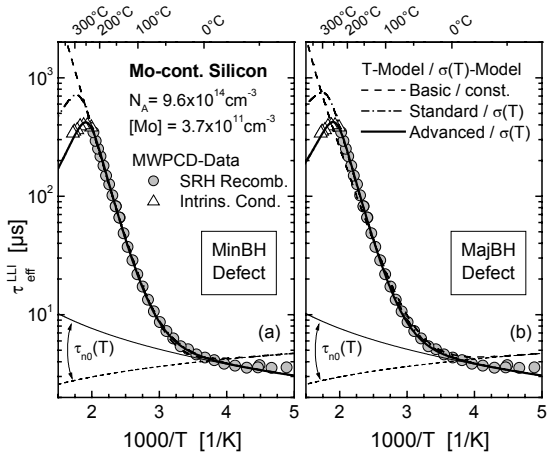

Figure 1: TDLS curve (symbols) measured on an intentionally Mo-contaminated Si-sample and different SRH simulations (lines). An accurate simulation of the low-temperature part below 300 K requires the insertion of a *T*-dependent capture cross section (thin solid line). An accurate simulation of the Arrhenius increase requires (b) for MajBH defects the $\sigma(T)$-model while (a) for MinBH defects σ=const. suffices. For an accurate modeling of the lifetime decrease above 500 K, induced by intrinsic conduction, not only the *T*-dependence of the majority carrier concentration (dash-dotted line) has to be considered but as well that of the band gap $E_{gap}(T)$ (solid line).

Further extensions of the SRH model arise from the attempt to model the *high-temperature part* of the TDLS curve. The observed lifetime decrease above 500 K originates from the abrupt onset of intrinsic conduction which leads to an exponential increase of the majority carrier concentration p_0 and thus to a strong decrease of the ratios n_1/p_0 and p_1/p_0, which stipulate SRH lifetime under low-level injection in that *T*-region. This explains that the SRH modeling using the basic *T*-model with temperature-independent equilibrium carrier concentrations $p_0=N_A$ and $n_0=n_i^2/N_A$, where n_i is the intrinsic carrier concentration at 300 K, does not even allow a qualitatively correct description in that *T*-region (dashed lines in Fig. 1). Analytically the temperature dependence of the equilibrium majority carrier concentrations is given by $p_0(T) = 1/2 \times [N_A+\{N_A^2+4\, n_i(T)^2\}^{1/2}]$ (see Ref. [7]). As can be seen from the dashed-dotted lines in Fig. 1, the introduction of this *standard T-model* allows a modeling of the $n_i(T)$-induced bent of the TDLS curve which is qualitatively correct though not quantitatively. The fact that the experimentally observed onset of intrinsic conduction is shifted to lower temperatures, implies a stronger *T*-dependence of $p_0(T)$ than assumed in the standard *T*-model.

This observation can be explained by a well-known effect: the temperature-induced narrowing of the silicon band gap. The reduction of $E_{gap}(T)$ with increasing temperature leads to an enhanced increase of $n_i(T)$ and $p_0(T)$, respectively, and thus induces an onset of the TDLS bent at lower temperatures. A well established model for the *T*-dependence of E_{gap} is found in Ref. [7]: $E_{gap}(T)=E_{gap}(0)-[\alpha T^2/(T+\beta)]$ with $E_{gap}(0)$=1.170 eV, $\alpha=4.73\times10^{-4}$ eV/K and β=636 K. The extraordinary performance of the SRH model being based on this *advanced T-model* is demonstrated by the solid lines in Fig. 1. As can be seen, both, the bent due to intrinsic conduction and the Arrhenius increase, are perfectly modeled as well for a MinBH as for a MajBH defect with an energy depth of 0.32 eV.

2.2 Transparent SRH analysis: defect-parameter-solution-surface (DPSS)

In order to quantify the accuracy of the defect parameters determined for the MinBH and the MajBH solution, the tolerance of the fitting model towards slight fluctuations of the fitting parameters has to be investigated. This investigation is performed with maximum transparency if the *defect-parameter-solution-surface* (DPSS) of the TDLS curve is determined. This new modeling procedure, in the following referred to as DPSS analysis, has recently been introduced in Ref. [4]. Using the SRH model which has been identified as optimum in the previous section, the DPSS diagram is determined from least squares fits of the measured TDLS curve for specified but gradually varied energy levels E_C-E_t of the defect center. The resulting symmetry factors *k* and the corresponding Chi^2-errors of the least squares fit are displayed in Fig. 2b and c as a function of the energy level E_C-E_t (solid lines). Both curves together represent the DPSS of the TDLS curve and are referred to as DPSS-*k* and DPSS-Chi^2 curve.

The practical value of the DPSS diagram consists in the fact that in general a comparison of the minimum values of the DPSS-Chi^2 curves allows the identification of the true band gap half of the defect center, while the width of each DPSS-Chi^2 curve makes an error estimation for the extracted defect parameters possible.

In the case of molybdenum the DPSS analysis shows that the solutions in the upper and the lower half of the band gap are identical in quality, which impedes the identification of the true band gap half and thus the identification of the *k*-factor. If a least squares error which is increased by a factor of 3 above its optimal value of 5.5×10^{-2} is defined as 'tolerable', the following ranges of acceptable values for the defect parameters can be deduced from the DPSS diagram (shaded areas in

Fig. 2b and c): for the MinBH solution E_C-E_t= 0.30..0.34 eV and k = 0.9..2.3 and for the MajBH solution E_t-E_V = 0.312..0.318 eV and k = 0.07..15. The qualitative shape of the DPSS curves directly reflects the fundamental difference between MinBH and MajBH defects discussed in Ref. [3]. The steep DPSS-k and the narrow DPSS-Chi^2 curve observed for the MajBH solution directly arise from the fact that the onset temperature of the Arrhenius increase is independent of k for a MajBH defect. Analogous, the existing k-dependence for a MinBH defect leads to a moderate slope of the DPSS-k curve and to a broader DPSS-Chi^2 curve. Thus, concerning accuracy, the defect parameters extracted from TDLS alone follow a pattern: for MinBH defects both defect parameters can be extracted with sufficient accuracy. MajBH defects on the contrary only allow an accurate E_t-determination while the k-determination in general fails, the extracted k-range being several orders of magnitude wide. Note that an upper bound for the k-factor of the MajBH solution is only found when the TDLS bent due to intrinsic conduction is considered and accurately modeled.

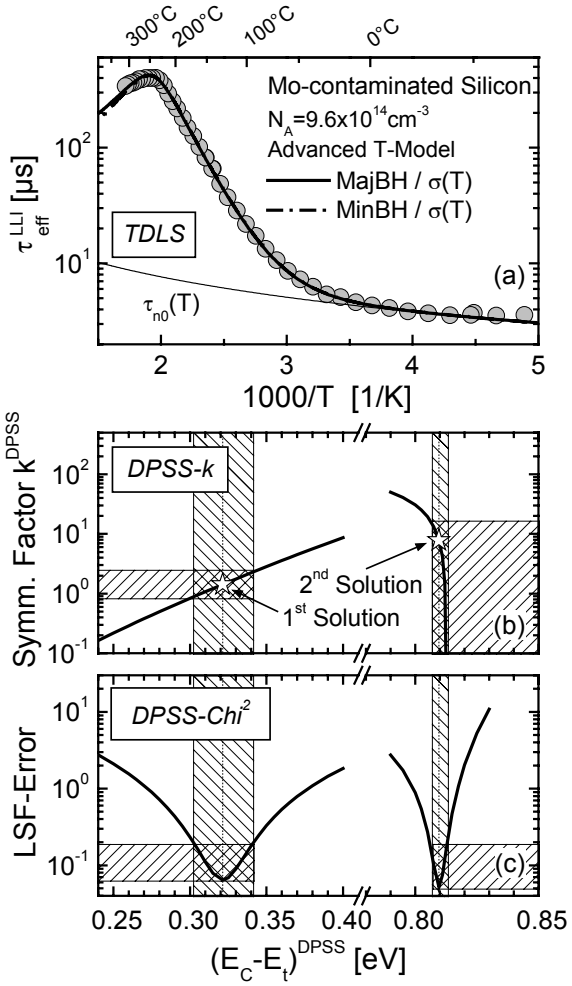

Figure 2: Advanced SRH analysis of the TDLS data from Fig. 1 by means of the 'defect parameter solution surface' (DPSS) associated with the optimum SRH model. While a comparison of the minimum values of the displayed DPSS-Chi^2 curves in general allows the identification of the true band gap half of the defect center, the width of each DPSS-Chi^2 curve makes an error estimation for the extracted defect parameters possible.

3. ADVANCED IDLS ANALYSIS

In order to reveal which of the two solutions obtained from the DPSS analysis of the TDLS curve provides the true defect parameters, the Mo-contaminated sample used for the TDLS investigation has been subject to an IDLS experiment. Figure 4 displays the IDLS curves measured by means of the quasi-steady-state photoconductance technique (QSSPC). As can be seen from Fig. 3, the accurate SRH modeling of the measured injection dependence in the whole injection range requires two independent SRH centers whose impact is displayed separately. While the increase of SRH lifetime up to Δn=2×10^{14} cm^{-3} is well described by only the deep defect level (dashed line) and is hardly affected by the shallow center (dash-dotted line), the successful modeling of the observed slight decrease of SRH lifetime under HLI conditions (above Δn=10^{15} cm^{-3}) strongly depends on the shallow defect level. Nevertheless, since TDLS is performed under LLI conditions, only the LLI-domination center is relevant for the comparison of IDLS and TDLS.

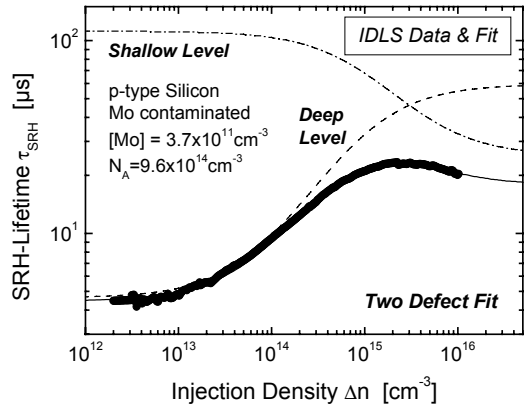

Figure 3: IDLS curve measured by means of the QSSPC technique on the same Mo-contaminated sample as investigated in Fig. 1. The accurate SRH modeling of the measured injection dependence in the whole Δn-range requires two independent SRH centers whose impact is displayed separately.

Concerning its applicability for defect characterization, IDLS faces the problem that the SRH parameterization of an IDLS curve is not unambiguous [2]. Thus, a detailed analysis of the IDLS data requires determining the 'Defect Parameter Solution Surface' which is associated with the defect center dominating the LLI part of the IDLS curve (see above). The resulting DPSS-k and DPSS-Chi^2 curve of the LLI-dominating defect center are displayed in Fig. 4 (dashed lines) together with the corresponding curves for the TDLS data (solid lines). A fundamental difference between the DPSS curves determined from the TDLS and IDLS data can be observed: while the DPSS-Chi^2 curves of the TDLS fits (solid line) show a pronounced minimum which indicates the best TDLS parameterization (E_C-E_t, k), the DPSS-Chi^2 curve of the IDLS curve (dashed line) is totally constant over a broad range of energy levels, which nicely shows that the defect parameters cannot be determined from only one IDLS curve.

4. COMBINED DPSS ANALYSIS

Beyond the instructive illustration of the SRH simulation, the combined DPSS diagram in Fig. 4, which contains the DPSS curves of the IDLS *and* TDLS measurement on the Mo-contaminated sample, allows an accurate determination of the defect parameters of molybdenum from the intersection points of the two DPSS-*k* curves related to the TDLS and IDLS curves. Since the DPSS-*k* curve associated with the TDLS curve contains solutions of varying accuracy, the quality of both DPSS-*k* intersection points significantly depends on their energy distance from the corresponding minimum of the DPSS-*Chi*^{2} curve related to TDLS. Since the DPSS-*k* intersection point in the upper half of the band gap strongly deviates from the corresponding DPSS-*Chi*^{2} minimum in terms of the energy position, the TDLS solution in the upper half of the band gap has to be rejected for reasons of inconsistency. In the lower half of the band gap on the contrary, the energy positions of both, the DPSS-*k* intersection point and the minimum of the DPSS-*Chi*^{2} curve, perfectly coincide. It can be concluded that the relevant molybdenum level is definitely located in the lower half of the band gap at E_t-E_V=0.317± 0.005 eV showing an electron/hole capture cross section ratio k=13±3. The quality of this finding is manifested in the high accuracy observed for the coincidence of the DPSS-*k* intersection point and the DPSS-*Chi*^{2} minimum.

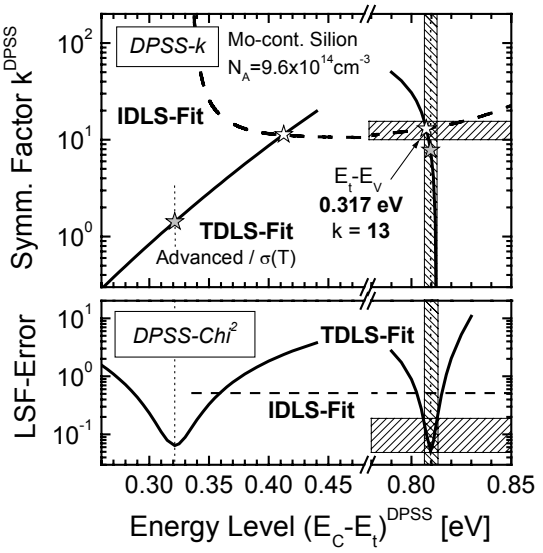

Figure 4: Superposition of the DPSS diagrams associated with the IDLS and TDLS curve of the Mo-contaminated sample displayed in Fig. 1 and 4, respectively. Unambiguous determination of both molybdenum defect parameters from the intersection point of the DPSS-*k* curves in the MajBH. The coincidence of this intersection point with the minimum of the DPSS-*Chi*^{2} curve manifests the accuracy of the determination and the necessity of the proposed extensions of the SRH model for the TDLS analysis.

The result is in good agreement with an energy level E_t-E_V=0.30 eV reported in literature for a molybdenum donor level [8]. This result was obtained from DLTS measurements which also led to a value for the hole capture cross section σ_p=6×10^{-16} cm^2 [8]. If this result is combined with the lifetime spectroscopic result for the symmetry factor k, a value of σ_n=(7.8±1.8)×10^{-15} cm^2 is determined for the unknown electron capture cross section of the molybdenum donor level.

5. CONCLUSION

The present investigation confirms that lifetime spectroscopy always allows a complete defect characterization on a single sample if TDLS and IDLS are combined. It is shown that an accurate modeling of the entire TDLS curve in an extended *T*-range from 130 to 580 K requires an advanced configuration of the SRH model to explain different superposed effects which have not been considered up to now but have a significant impact on the spectroscopic result. Under low temperatures the accurate modeling in general requires a $\sigma(T)$-model which can directly be determined from the low-temperature part of the TDLS curve and thus provides an additional fingerprint of the defect. Under high temperatures an accurate modeling of the TDLS bent due to intrinsic conduction is only achieved if the temperature dependence of both, the equilibrium carrier concentrations $p_0(T)$, $n_0(T)$ and the band gap $E_{gap}(T)$, are considered.

Beyond these physical extensions of the LS analysis, the new LS modeling procedure consisting in the determination of the *defect-parameter-solution-surface* (DPSS) is further extended to be applicable to defect levels in either band gap half. Perfectly visualizing the ambiguity of the SRH parameterization of a single IDLS curve, the newly developed DPSS diagram makes it possible to assess the accuracy and consistency of the spectroscopic results obtained from TDLS and IDLS by a simple analysis of the intersection points of the associated DPSS curves. The transparency achieved for the SRH modeling makes the DPSS analysis proposed a versatile tool for data evaluation in lifetime spectroscopy, which may set a new standard.

The application of this advanced LS analysis on a pair of TDLS and IDLS curves measured on an intentionally Mo-contaminated silicon sample demonstrates the excellent performance of lifetime spectroscopy. In good agreement with DLTS results from literature, the combined DPSS analysis of TDLS and IDLS consistently identifies a known molybdenum donor level at E_t-E_V=0.317 eV as the level with highest recombination activity. Moreover, the study reveals an enhanced electron capture cross section (k=13), which is determined at σ_n=7.8×10^{-15} cm^2, and thus completes the knowledge on the defect properties. Allowing the exact determination of E_t and k, advanced lifetime spectroscopy provides a full picture of how the molybdenum defect affects cell performance.

In conclusion, the methodological and experimental results of the present work demonstrate that in terms of both, the physical understanding and the implementation, lifetime spectroscopy is ready to be applied as a highly sensitive diagnostic tool in the semiconductor industry.

ACKNOWLEDGEMENTS

The authors would like to thank P. Lichtner and E. Tavaszi for lifetime measurements. This work has been supported by the German Federal Ministry of the

Environment, Nature Conservation and Nuclear Safety (BMU) under contract number 01SF0010.

REFERENCES

[1] W.M. Bullis and H.R. Huff, J. Electrochem. Soc. **143** (4), 1399-405 (1996).

[2] S. Rein, T. Rehrl, W. Warta, and S.W. Glunz, J. Appl. Phys. **91** (3), 2059-2070 (2002).

[3] S. Rein, P. Lichtner, W. Warta, and S.W. Glunz, *Proc. 29th IEEE PVSC* (New Orleans, Louisiana, 2002), p. 190.

[4] S. Rein and S.W. Glunz, Appl. Phys. Lett. **82** (7), 1054-56 (2003).

[5] M. Lax, Phys. Rev. **119** (5), 1502-23 (1960).

[6] A. Hangleiter, Phys. Rev. B **35** (17), 9149-61 (1987).

[7] S.M. Sze, *Physics of Semiconductor Devices*, 2nd Edition (John Wiley & Sons, New York, 1981).

[8] L.Börnstein, *Semiconductors* (Springer-Verlag, Berlin, 2002).